Advances in Engineering Research, volume 146

4th International Conference on Material Engineering and Application (ICMEA 2017)

Hydrothermal Synthesis of Clew-like $Bi_2Sn_2O_7$ and Visible-light Photocatalytic Activity

Wei Huang[1]
[1]School of Materials Science and Engineering, Guilin University of Electronic Technology, Guilin 541004, P.R. China

Chaohao Hu[1,2,*]
[1]School of Materials Science and Engineering, Guilin University of Electronic Technology, Guilin 541004, P.R. China.
[2]Guangxi Key Laboratory of Information Materials, Guilin University of Electronic Technology, Guilin 541004, P.R. China
E-mail: chaohao.hu@guet.edu.cn;

Binqing Zhu[1]
[1]School of Materials Science and Engineering, Guilin University of Electronic Technology, Guilin 541004, P.R. China

Yan Zhong[1,2,*]
[1]School of Materials Science and Engineering, Guilin University of Electronic Technology, Guilin 541004, P.R. China
[2]Guangxi Key Laboratory of Information Materials, Guilin University of Electronic Technology, Guilin 541004, P.R. China.
E-mail: yanzhong@guet.edu.cn

Huaiying Zhou[1,2]
[1]School of Materials Science and Engineering, Guilin University of Electronic Technology, Guilin 541004, P.R. China
[2]Guangxi Key Laboratory of Information Materials, Guilin University of Electronic Technology, Guilin 541004, P.R. China

***Abstract*—Visible-light responsive bismuth pyrostannate ($Bi_2Sn_2O_7$) photocatalysts with the clew-like morphology have been synthesized by the hydrothermal method. XRD, FE-SEM, BET, UV-vis DRS was used to characterize the phase structure, surface morphology, and optical properties of catalysts. When the hydrothermal time was 24 h, the prepared catalysts exhibited the best photocatalytic activity and the photodegradation efficiency of rhodamine B (RhB, 5 mg/L) was about 87% after 240 min visible-light illumination. The recycle experiments show that the prepared clew-like $Bi_2Sn_2O_7$ photocatalysts possess excellent repeatability and stability.**

Keywords-$Bi_2Sn_2O_7$; Hydrothermal method; Photocatalytic Activity; Visible light response.

I. INTRODUCTION

Semiconductor photocatalytic technology has been widely used in environmental remediation and clean hydrogen energy production since the photocatalytic activity of TiO_2 was first reported by Fujishima and Honda in 1972 [1]. Currently, TiO_2 has been widely investigated as one of the best photocatalysts for the oxidative decomposition of organic pollutants because of its outstanding oxidative power, high stability, nontoxicity, and photostability [2-8]. However, TiO_2 is only active under UV light irradiation due to its large band gap of about 3.2 eV, which limits its further application in the visible-light region [9, 10]. It is important to explore new photocatalysts responsive to visible-light irradiation for improving the photocatalytic activity. In the past few decades, many researchers have focused their efforts on the visible-light-driven semiconductor photocatalysts containing bismuth with high activities for degrading organic contaminants and water splitting such as $BiVO_4$ [11], Bi_2WO_6 [12], BiOCl [13], $CaBiO_2Cl$ [14], $Bi_2O_2CO_3$ [15] and $Bi_xO_yI_z$ [16]. $Bi_2Sn_2O_7$ (BSO) has also attracted the interest of many researchers due to various physical and chemical properties. BSO belongs to the pyrochlore family of general formula $A_2B_2O_7$, where A cations

are eight-coordinated and B cations are six-coordinated [17]. Recently, Xu et al. [18] have achieved the pyrochlore-type BSO nanoparticles and investigated its photocatalytic performance. Wu et al. [19] have synthesized nano-BSO by a hydrothermal method and studied the photocatalytic activity in the degradation of methyl orange.

In this study, BSO was successfully synthesized by additive-free hydrothermal processes in a wide range of reaction time. The effects of hydrothermal time on crystal structure, morphologies, particle sizes and optical properties were investigated. Photocatalytic activity of clew-like BSO was evaluated by degradation of rhodamine B (RhB) under visible light irradiation.

II. EXPERIMENTAL PROCEDURES

A. Synthesis

All chemicals were obtained commercially and used without further purification. In a typical hydrothermal processing, 0.01 mol of Bi(NO3)3·5H2O was dissolved in 5 mL HNO3 with the concentration of 2 mol/L and stirred for 10 min at room temperature to get solution A, 0.01 mol of SnCl4·5H2O was dissolved in 20 mL deionized water and also stirred for 10 min at room temperature to get solution B. Then solution B was poured into solution A under vigorous stirring and the pH value of the mixture was adjusted to 13 by using 4 mol/L of NaOH. The mixed solution was stirred continuously at room temperature for 30 min and then transferred into Teflon-lined autoclave (100 mL capacity, 60% full) and kept at 200 oC for 3, 6, 12, 24, 48 h in an oven, respectively. After the reaction, the resulting yellow powders were obtained by filtration and washing with absolute ethanol and deionized water several times. The final products were dried at 60 oC for 16 h in an oven. The obtained powders were correspondingly labeled as BSO-3, BSO-6, BSO-12, BSO-24, and BSO-48 according to the above time of hydrothermal reaction.

B. Characterization

The XRD patterns of as-prepared samples (2θ, range from 10º to 80º) were recorded at room temperature with scanning speed of 5º min−1 using Cu Kα radiation (λ = 0.1541 nm) from a 40 kV X-ray source (Bruker D8-Advance XRD, Germany). Field emission scanning electron microscopy (FE-SEM, Quanta 450 FEG, USA) was used to characterize the morphology and microstructure. The composition of the samples was examined using energy dispersive X-ray detector (EDS, Thermo Noran VANTAG-ESI, USA). The Brunauer-Emmett-Teller (BET) specific surface areas of the materials were detected by Quantachrome ASIQM0002-4 nitrogen adsorption apparatus. Fourier transform infrared (FT-IR) spectra was recorded on FTIR spectrometer (Thermo Fisher Nicolet 6700) using the standard KBr disk method. The optical properties of the photocatalysts were checked on an UV-vis spectrometer (Puxi TU-1901, Beijing) in the range of 220-750 nm. UV–vis diffuse reflectance spectra (UV–vis DRS) of the catalysts were determined with a Puxi TU-1901 spectrophotometer using BaSO4 as a reference.

C. Photocatalytic Activity Test

The photocatalytic efficiencies of the prepared BSO were evaluated through degrading RhB under visible-light irradiation at room temperature. An amount of 0.20 g powder of photocatalyst was immersed in a quartz beaker containing 100 mL of RhB solution with a concentration of 5 mg/L. In order to ensure adsorption/desorption equilibrium between RhB and photocatalyst, the suspension was stirred in the dark for 30 min. 300 W Xeon arc lamp was used as the light source with a 420 nm cut of filter, which was placed at about 10 cm from the reactor. After the photocatalytic reactions, 6 mL of suspension was taken out at given time intervals. At last, a centrifuge was used to remove the powder and the supernatant was taken for analysis. The absorbance of centrifugal solution was determined at 553 nm by UV-vis spectrophotometer.

III. RESULTS AND DISCUSSION

A. Structural and Morphological Characterization

The phase and composition of the samples were characterized by XRD. Figure 1 shows the XRD patterns of BSO powders at different hydrothermal time. It can be seen that reaction time has great influence on the crystallization of BSO. For the sample BSO-3, the main diffraction peaks appeared at 2θ = 28.8°, 33.3°, 47.9°, 56.9°, which can be indexed to a pure cubic phase of BSO (JCPDS no. 87-0284). However, other peaks which belong to Bi2O2.3 can also be observed. After increasing the reaction time to 6 h, no other peaks can be observed, indicating high purity of the final products. With the treatment time going up to 12 or 24 h, the peaks are more strong and sharp. However, the main diffraction peaks become slightly declined when the hydrothermal time is increased to 48 h.

The IR spectra of the BSO samples derived from different hydrothermal time are shown in Figure 2. The bands at around 2920 and 2850 cm-1 can be assigned to aliphatic C-H [20]. The medium peaks at about 1390 and 1440 cm-1 are ascribed to the adsorbed trace NO3-. The bands centered at about 3415 and 1630 cm−1 are assigned to O-H stretching and bending modes of water, respectively [21]. The band at about 600 cm−1 is ascribed to the Sn-O stretching vibration in the SnO6 octahedron and the Bi-O stretching vibration centered at about 500 cm−1 is consistent with the previous data [22,23]. As shown in Figure 2, moreover, the samples show

stronger peaks and a slight blue shift at the bands around 625 and 513 cm−1 with increasing the hydrothermal time, which is attributed to the Sn-O and Bi-O stretching vibrations and further confirms the changes of crystal structure.

The typical FE-SEM images of BSO obtained at different hydrothermal time are displayed in Figure 3. Obviously, the hydrothermal time has a great effect on the surface morphology and texture of products. As shown in Figure 3(a), the clew-like morphology has emerged in BSO-3, which mostly consists of microspheres with a diameter of 8-12 μm and a small amount of irregular block structure. It can be found from Figure 3(b) and 3(c) that the crystallites of clew-like BSO become better with increasing the hydrothermal time to 6 and 12 h. As shown in Figure 3(d) and 3(e), especially, the sample of BSO-24 shows the almost perfect clew-like morphology. The morphology of BSO-48 changed a lot and some clew-like microspheres are broken after the reaction time is increased to 48 h (Figure 3(f)).

The BET surface area and pore structure of the as-prepared BSO-12 and BSO-24 photocatalysts were characterized using nitrogen adsorption-desorption measurements as depicted in Figure 4. It can be seen that the isotherms of two samples are of classical type IV according to the IUPAC classification, indicating the characteristics of mesoporous materials. Compared to the BSO-12 sample, the measured BET surface area of the BSO-24 sample is about 27.1 m2/g and larger than that of BSO-12 (17.2 m2/g). In addition, according to the pore size distribution curves shown in Figure 4, the pore size of BSO-24 determined by BJH (Barrett-Joyner-Halenda) method is about 14.02 nm and obviously larger than that of BSO (8.06 nm). The mesopores can easily capture photogenerated electrons and holes, suppressing the recombination of electron-hole pairs and this could be beneficial for the photocatalytic activity enhancement.

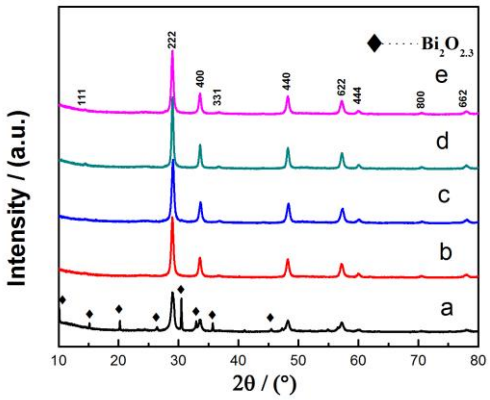

Figure 1. XRD patterns of BSO powders prepared at different hydrothermal times: (a) BSO-3, (b) BSO-6, (c) BSO-12, (d) BSO-24, (e) BSO-48

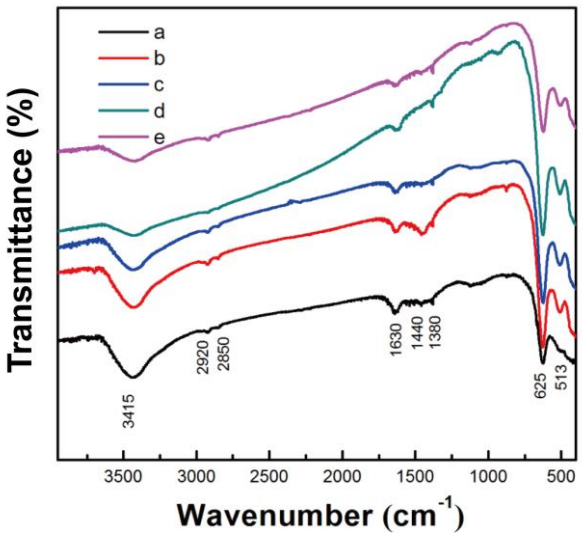

Figure 2. IR spectra of the as-prepared BSO powders at different hydrothermal time: (a) BSO-3, (b) BSO-6, (c) BSO-12, (d) BSO-24, (e) BSO-48

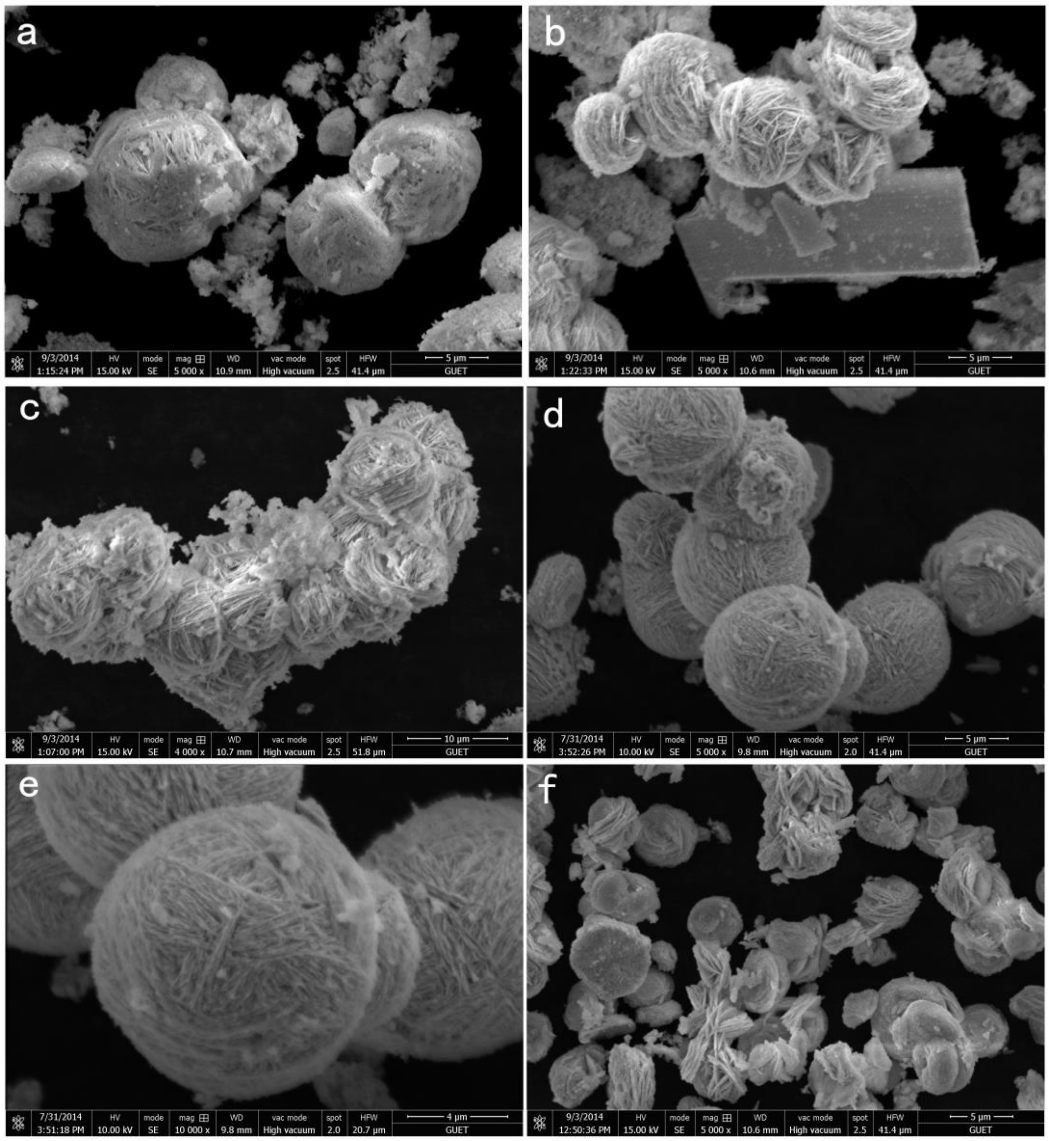

Figure 3. Typical FE-SEM images of BSO obtained at different hydrothermal time: (a) BSO-3, (b) BSO-6, (c) BSO-12, (d)-(e) BSO-24, (f) BSO-48

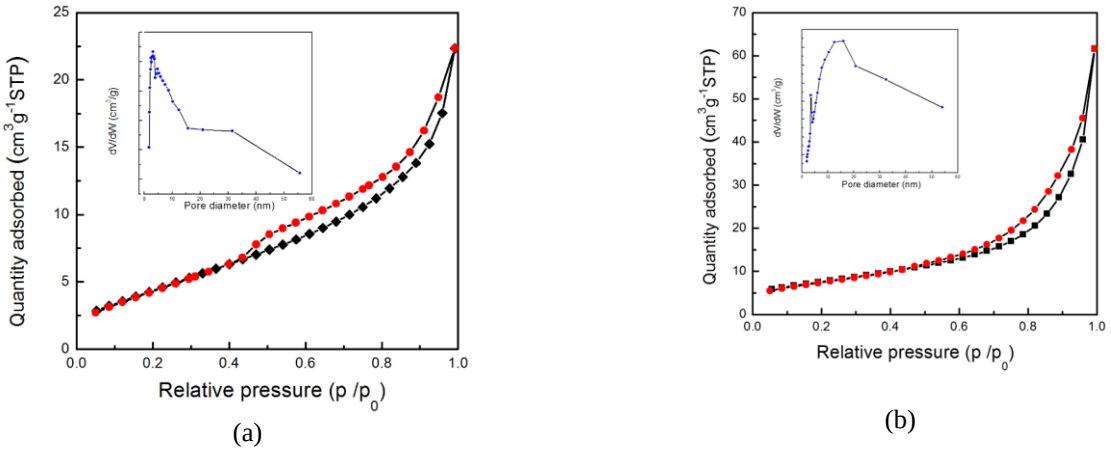

Figure 4. The N2 sorption isotherms and pore width distribution of as-synthesized samples measured using BJH method: (a) BSO-12, (b) BSO-24

B. UV–visible Absorption Spectra

The optical absorption properties of semiconductor materials are related to the electronic structure and considered to be the key factor in determining the photocatalytic activity. Figure 5(a) represents the UV-vis diffuse reflectance spectra of the clew-like BSO samples. Apparently, the steep shape of the spectra indicates that the visible light absorption is due to the band gap transition and all the samples show the excellent visible-light absorption around 450 nm. For a crystalline semiconductor, the optical band edge can be obtained from the following equation:

$(\alpha hv)n = A (hv - Eg)$

Where α, A, hv, and Eg are the absorption coefficient, a constant, the absorption energy, and band gap. Here n depends on the characteristic of the transition in a crystalline semiconductor. For BSO, the value of n is 1/2 for the indirect transition. The Eg of BSO can be estimated from a plot of $(\alpha hv)1/2$ versus the photon energy hv shown in Figure 5(b). The band gap absorption edge of BSO-24 is about 495 nm and the estimated Eg is about 2.50 eV, which is similar to the previously reported value [24]. The Eg of other four samples (BSO-3, BSO-6, BSO-12, BSO-48) are about 2.59, 2.81, 2.85, and 2.56 eV, respectively.

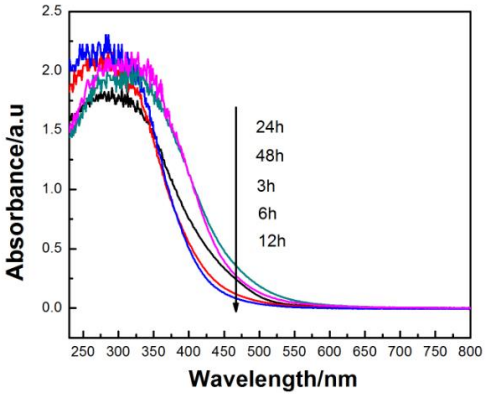

(a)

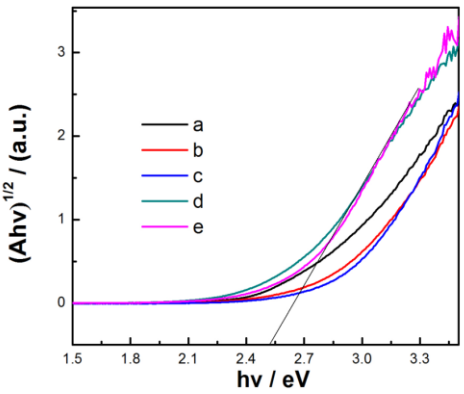

(b)

Figure 5. (a) UV-Vis difuse relectance spectra and (b) plots of (αhv)1/2 versus photon energy of the BSO samples prepared at different hydrothermal time

C. Photocatalytic Activity

The photocatalytic performance of BSO is evaluated by the degradation of RhB (5 mg/L) under visible-light irradiation. Figure 6(a) and 6(b) show the temporal evolution of the spectral changes during the photodegradation of BSO-3 and BSO-24 under visible-light illumination. The intensity of the main absorption peaks of RhB at 553 nm decrease gradually as the irradiation time increases, indicating the excellent photocatalytic activity of samples. The degradation efficiencies of RhB in presence of BSO prepared at different hydrothermal time are shown in Figure 6(c). BSO-24 shows the best photocatalytic efficiency and about 87% of RhB is degraded after 240 min illumination, which could be related to its high crystallinity, large BET surface area, and good visible-light response as stressed in the above analysis. In addition, the good repeatability and stability of a photocatalyst are significant to evaluate the catalyst for practical application. The stability of BSO-24 was investigated by the cycling runs for degradation of RhB under visible light illumination and the measured results are presented in Figure 6(d). The sample of BSO-24 was regenerated in every 240 min via a series of steps including centrifuge separating, washing, and drying at 60oC for 12 h. As shown in Figure 6(d), no apparent deactivation of photocatalyst can be seen after four cycling runs. Furthermore, According to our measurements of XRD and FE-SEM on BSO-24 after the four recycling tests, there are no observable changes in its morphology and microstructure as well as the crystal structures. As a result, the prepared BSO-24 possesses good repeatability and stability and is not prone to light corrosion during the degradation process.

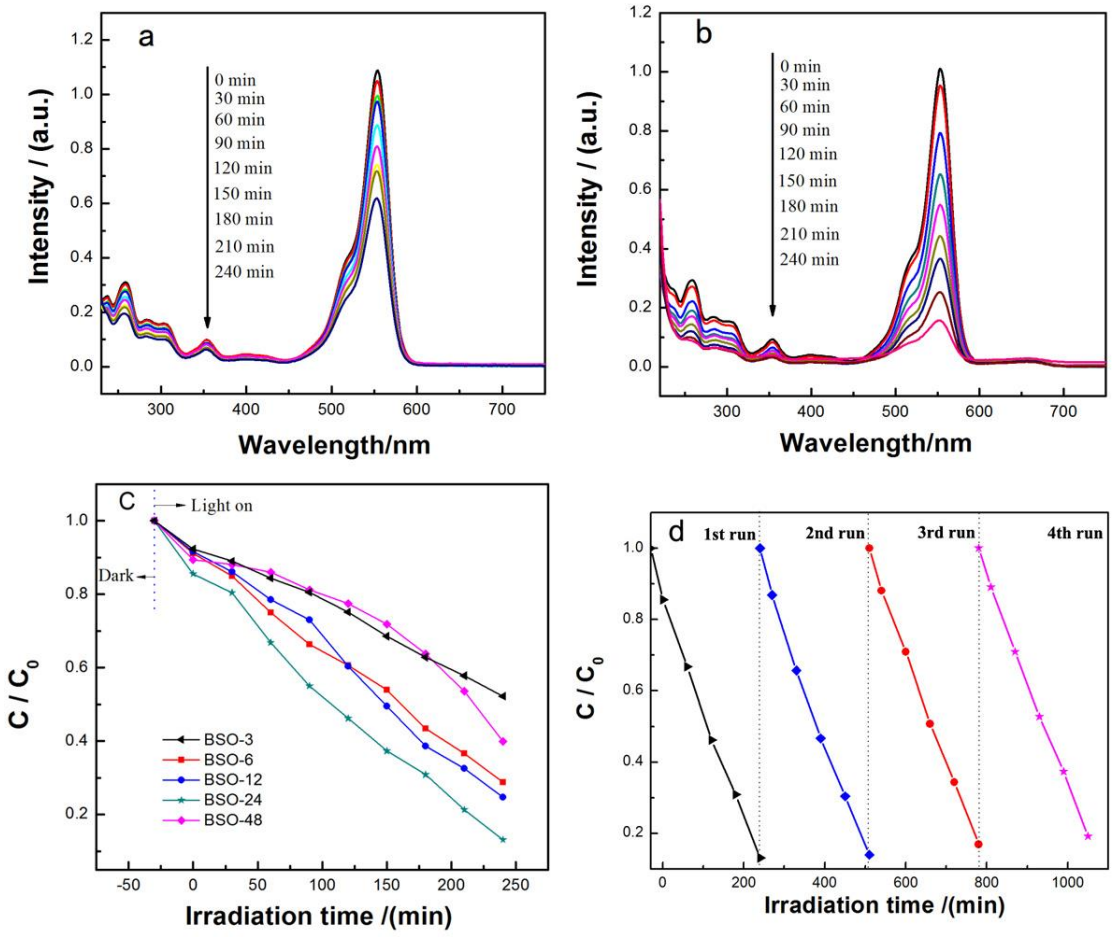

Figure 6. Absorbance changes of RhB dye solution in (a) BSO-3 and (b) BSO-24; (c) photocatalytic degradation of RhB as a function of irradiation time; (d) cycling runs in the photodegration of RhB using BSO-24.

IV. CONCLUSION

In summary, the clew-like BSO photocatalysts have been prepared successfully by a hydrothermal method. The results reveal that the hydrothermal time has a great effect on the crystalline, morphology, band gap, adsorptive behavior and photocatalytic performances of the as-synthesized BSO. When the hydrothermal time is 24 h, the prepared BSO shows the best photocatalytic performance due to its better crystalline quality, surface morphology and texture, intensive absorption within the visible light range and specific surface area. Moreover, the clew-like BSO photocatalysts show good photocatalytic repeatability and stability.

ACKNOWLEDGEMENT

The authors gratefully acknowledge the financial support from the National Basic Research Program of China (Grant No. 2014CB643703), the National Natural Science Foundation of China (Grant No. 11464008 and No. 51401060), the Guangxi Natural Science Foundation (Grant No. 2014GXNSFGA118001 and 2016GXNSFGA380001).

REFERENCES

[1] Fujishima A and Honda K 1972 *Nature* **238** 37

[2] Yu K, Yang S G, He H and Sun C 2009 *J Phys. Chem.* **113** 10024

[3] Zhang C and Zhu Y F 2005 *Chem. Mater.* **17** 3537

[4] Liu H, Wu Y and Zhang J. 2011 *ACS Appl. Mater. Interfaces* **3** 1757

[5] Zhang Z J, Wang W Z and Shang M 2010 *Catal. Commun.* **11** 982

[6] Kikugawa N, Yang L Q, Matsumoto T and Ye J H 2010 *J. Mater. Res.* **25** 177

[7] Zhang L S, Wang H L and Chen Z G 2011 *Appl. Catal. B: Environ.* **106** 1

[8] Linsebigler A L, Lu G Q and Yates J T 1995 *Chem. Rev.* **95** 735

[9] Kohtani S, Hiro J, Yamamoto N and Kudo A 2005 *Catal. Commun.* **6** 185

[10] Zhang S, Zhang C, Man Y and Zhu Y F 2006 *J. Solid State Chem.* **179** 62

[11] Kudo A, Omori K and Kato H 1999 *J. Am. Chem. Soc.*

121 11459

[12] Tang J, Zou Z and Ye J 2004 *Catal. Lett.* **92** 53

[13] Zhang K L, Liu C M, Huang F Q, Zheng C and Wang W D 2006 *Appl. Catal. B: Environ.* **68** 125

[14] Shi R, Xu TG, Zhu Y F and Zhou J 2012 *CrystEngComm* **14** 6257

[15] Madhusudan P, Yu J G, Wang W G, Cheng B and Liu G 2012 *Dalton Trans.* **47** 14345

[16] Liu C H and Zhang D 2015 *Appl. Phys. A: General* **3** 913

[17] Bala I, Barbar S K and Roy M 2012 *Physica B* **407** 3939

[18] Xu W C, Liu Z and Fang J Z 2013 *Int. J. Photoenergy* **7** 394079

[19] Wu J J, Huang F Q and Lu X J 2011 *Mater. Chem.* **21** 3872

[20] Ke D, Peng T, Ma L, Cai P and Dai K 2009 *Inorg. Chem.* **48** 4685

[21] Min Y L, Zhang K, Chen Y C and Zhang Y G 2012 *Sep. Purif. Technol.* **86** 98

[22] Subramanian M A, Aravamudan G and Subba Rao G V 1983 *Indian Acad. Sci.* **2** 55

[23] Pascuta P and Culea E 2008 *Mater. Lett.* **25** 4127

[24] Tian Q F, Zhuang J G and Wang J X 2012 *Appl. Catal. A: General* **425– 426** 74